CHAPTER 4

ANALYSIS AND PROCESSING

4.1 The relationships between meteorological parameters and soil gas radon concentrations

An understanding of the interactions of meteorological variables with soil gas radon is necessary if radon concentration is to be used to predict earthquakes. The data used to compare meteorological and radon values are shown in Figures 4.1a, 4.1b, and 4.1c.

These observations found that radon concentration depends on all meteorological parameters at the same time. So it is difficult to determine the correlation of radon anomalies to each meteorological parameter, or from other effects, such as earthquakes. In order to use radon anomalies as a precursor for earthquake prediction, the correlation of radon concentration with the three meteorological parameters, soil temperature, precipitation, and barometric pressure, separately and the correlation with these three parameters combined, must be determined. The next section shows the mathematical process used for estimation in radon time series of the three meteorological parameters separately and of the three meteorological parameters combined. Then the overall effect of all parameters on radon anomalies will be separately analyzed.

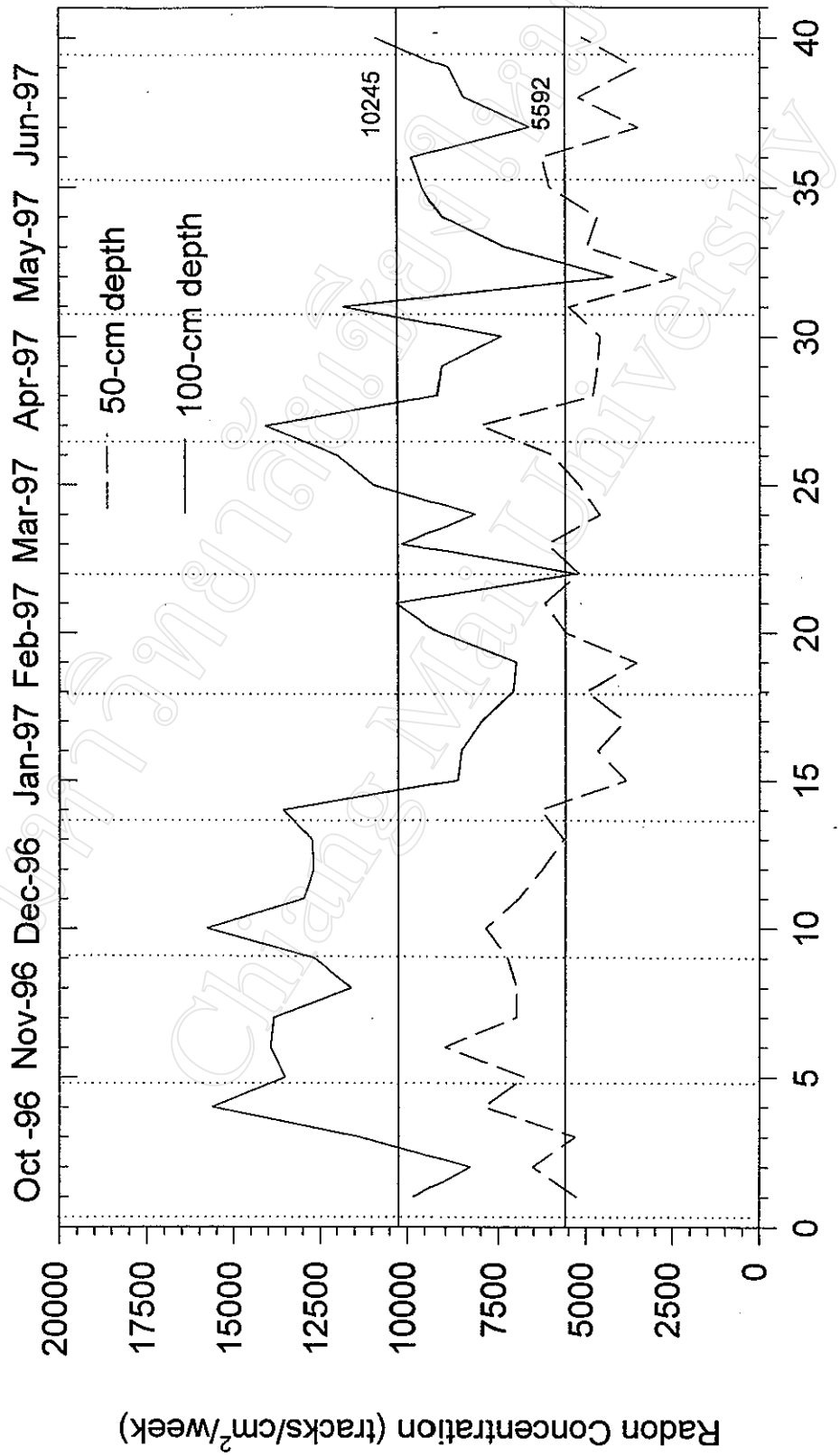

Figure 4.1a Average radon concentration at two depths.

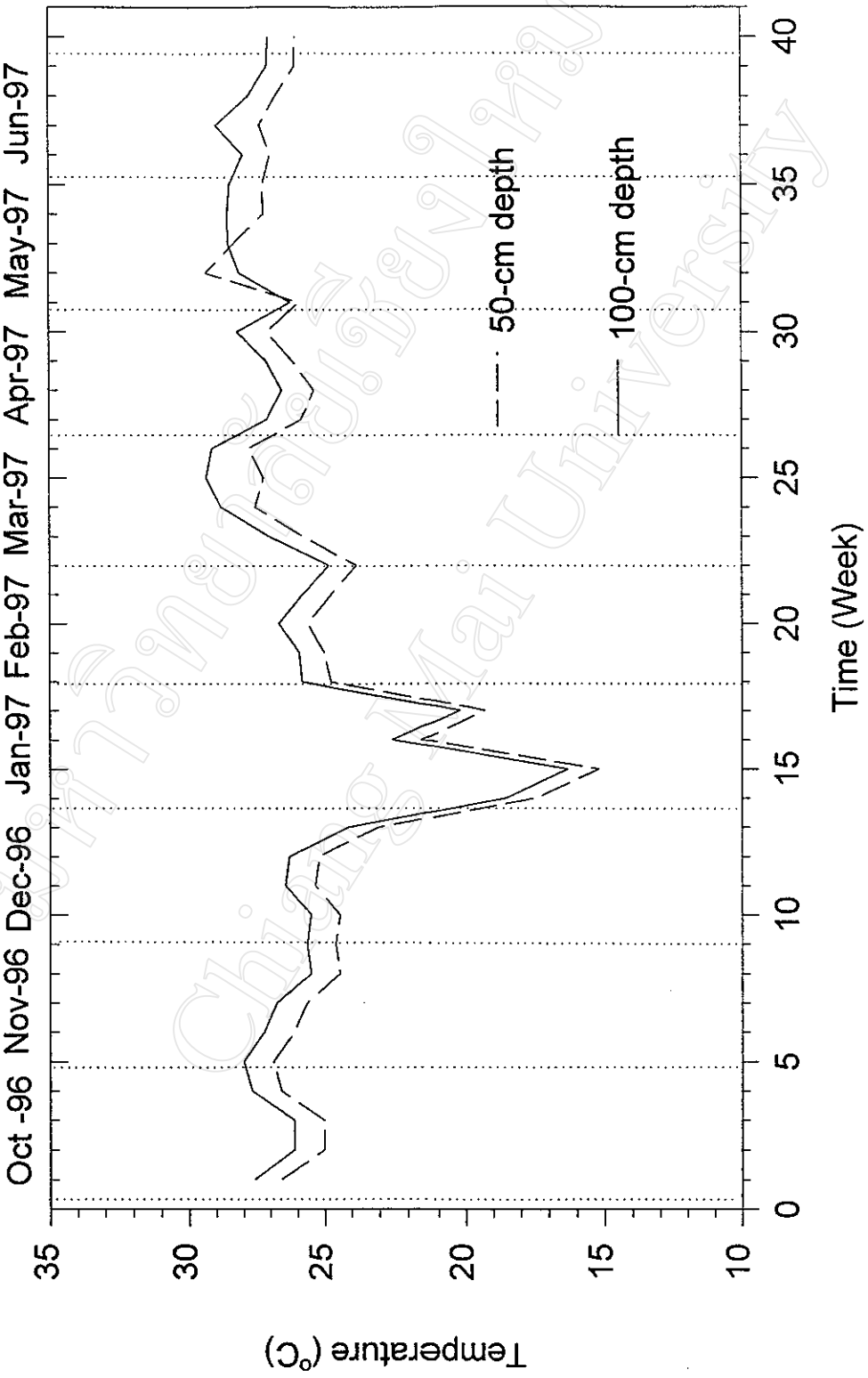

Figure 4.1b Average soil temperature at two depths.

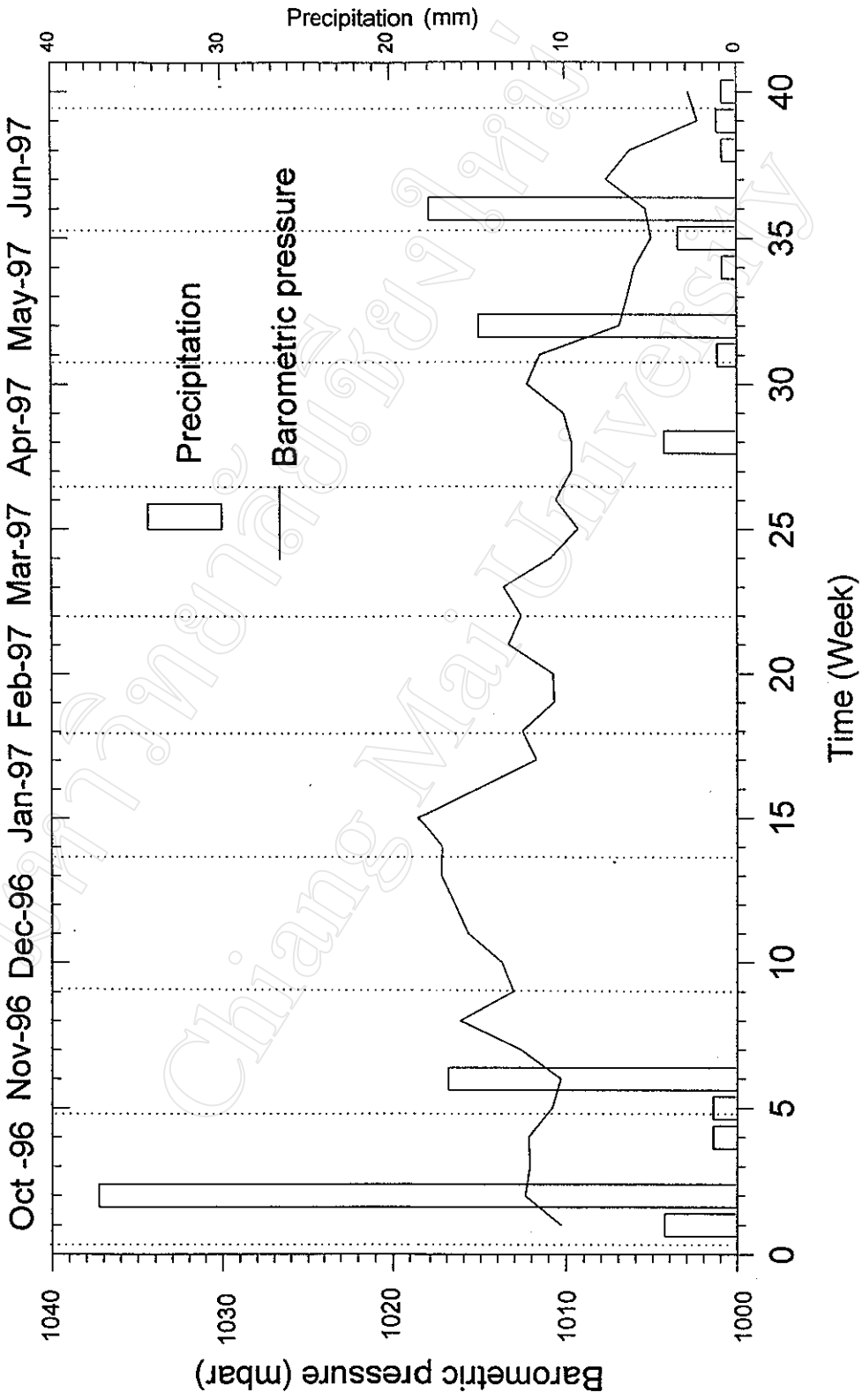

Figure 4.1c Average barometric pressure and precipitation.

4.2 Data processing of soil gas radon

The observed variations of radon concentration consist of the fluctuation of radon due to meteorological parameters (precipitation, soil temperature, and barometric pressure) and the variation of radon due to unpredictable events (earthquakes). In order to distinguish the variation of radon concentration due to meteorological parameters from the total radon anomaly, the mathematical model of Pinault was used in this study. This model is :

$$Y(n) = Y'(n) + \Psi(n)$$

$$Y(n) = \Gamma_1 * X_1(n) + \Gamma_2 * X_2(n) + \Gamma_3 * X_3(n) + \Psi(n)$$

$$Y(n) = \underline{\Gamma}_p \underline{X}_p(n) + \Psi(n)$$

$$Y(n)\, \underline{X}^T_p(n) = \underline{\Gamma}_p \underline{X}_p(n)\, \underline{X}^T_p(n)$$

$$\underline{\Gamma}_p = \{Y(n)\, \underline{X}^T_p(n)\}\{\underline{X}_p(n)\, \underline{X}^T_p(n)\}^{-1}$$

where, $Y(n)$ is the time series of average radon concentration in one week,

$Y'(n)$ is the time series of average radon concentration related to meteorological parameters in one week,

$\underline{\Gamma}_p$ is the impulse response of order p,

$\Psi(n)$ is the time series of average radon concentration due to unpredictable events,

$X_1(n)$, $X_2(n)$, and $X_3(n)$ are the time series of average soil temperature, barometric pressure, and rainfall in one week, respectively,

and n is a discrete time (week), n=1,2,...,40.

The conditions for solving Γ are as follows:

a) Y(n) linearly correlated to meteorological parameters,

b) Ψ(n) not correlated to any meteorological parameters,

c) Least square method is use for the best estimator of Γ.

The processing outlined in Figure 4.2a was used for separating the interaction of meteorological parameters on radon concentration from the total radon anomaly. The input data of Program 1 are shown in Table A6 and the results of processing are shown in Figures 4.2b.

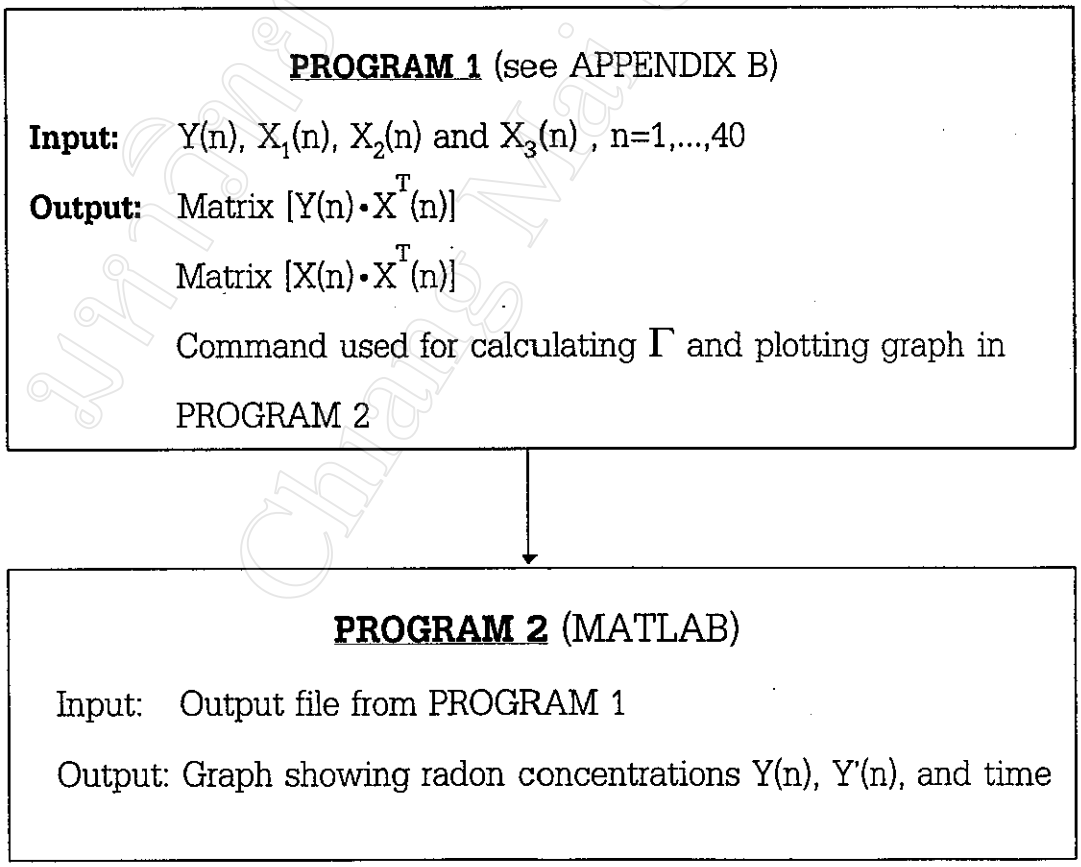

Figure 4.2a Outline of Processing.

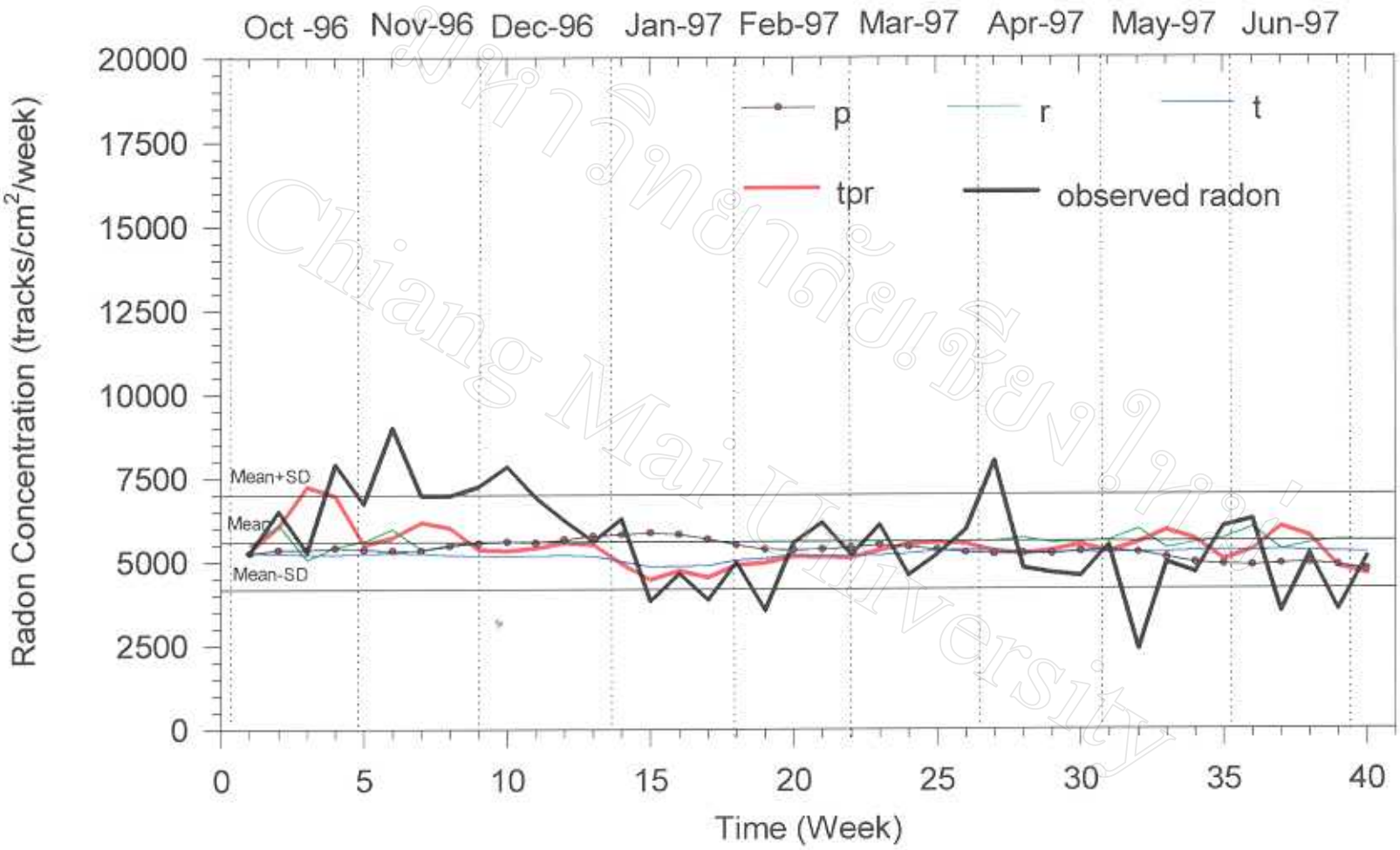

Figure 4.2b Calculated and observed radon time series at 50-cm depth.

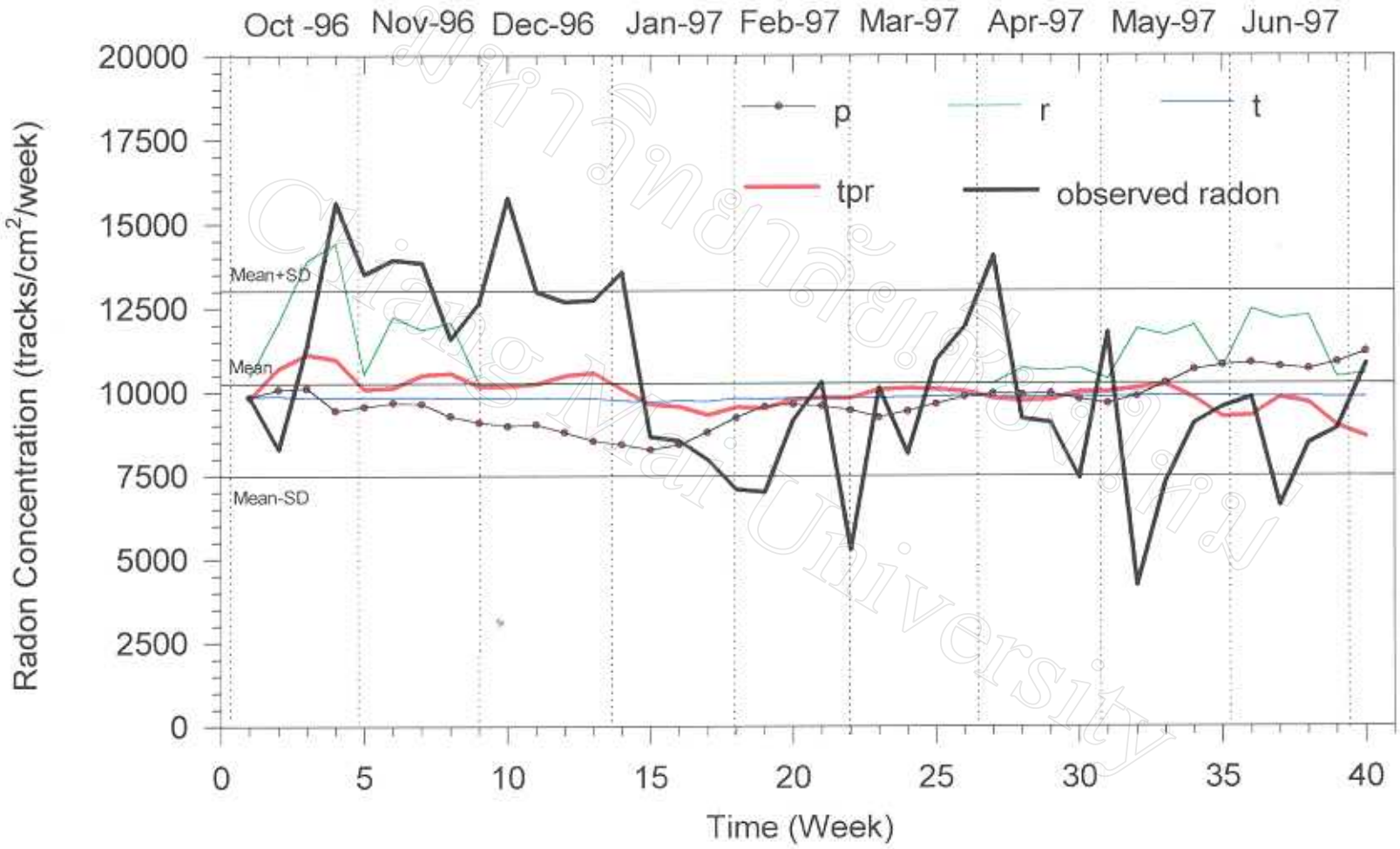

Figure 4.2c Calculated and observed radon time series at 100-cm depth.

Figure 4.2b, and 4.2c show the estimation of radon signal due to meteorological parameters (r, t, p, and tpr are the average radon time series due to precipitation, soil temperature, barometric pressure, and all of these meteorological parameters) and average radon time series from the observation. The estimated radon at 50-cm depth is closer to the observed radon than at 100-cm depth, since the meteorological parameters affected the soil gas radon concentration at the 50-cm depth more than at the 100-cm depth. The meteorological parameters are related to radon data both separately and combined. Long-term radon variations were governed by barometric pressure and soil temperature and that short-term fluctuations were controlled by precipitation. In the past the over-all increase in radon concentration due to the meteorological parameters is always less than standard deviation(Virk 1994) that conform with these estimation. However, sometimes the estimation of radon signal due to these meteorological parameters agrees with the observed radon data and sometimes it disagrees with the observed radon data. These variations in agreement may be from other reasons and are discussed in section 4.3.

4.3 Comparison of radon anomaly and earthquakes data

In this section, the dislocation model of Fleischer (Fleischer, 1981) was used to select some earthquakes associated with radon anomalies. This dislocation model relates the maximum distance from a radon monitoring site to the earthquake magnitude for a quake that shows a clear change in radon concentration. This relationship can be written as:

$$X_m = 10^{0.813M}/16.6 \text{ for } M \leq 3$$

$$X_m = 10^{0.48M}/1.66 \text{ for } M \geq 3 \qquad (17)$$

where, X_m is maximum distance from an earthquake epicenter to a radon detector (km),

M is magnitude of earthquake (Richter).

Equation 17 is plotted in Figure 4.3a, the solid line being the calculated value of the maximum distance at which an earthquake of a given magnitude should be able to affect radon concentration. These lines are calculated events from many parts of the world which had radon anomalies. For comparison, Figure 4.3a shows some of Fleischer (1981) data and data from this study. If equation 17 was both rigorous and relevant, no earthquake event that had radon anomaly should fall above the values given by equation 17. In fact some events, which showed radon anomalies before earthquakes, lie above the curve, but only slightly above and certainly well within the approximations made.

When comparing the events observed during this study with equation 17 in Figure 4.3a, only two events from 40 earthquakes are below the curve. However, some events are only slightly above the curve and should be associated with earthquakes.

When the weekly integrated radon data in Figure 4.3b are compared with the 43 earthquakes in Figure 3.1i, two radon anomalies at two depths clearly correspond to two earthquakes. The first anomaly occurred about three weeks at 100-cm depth and about one week at 50-cm depth before the 6.2M earthquake in Myanmar, 293.44 km from the radon monitoring site. The second anomaly occurred about three weeks at two depths before the 5.5M earthquake along the Thai-Laos border, 159.41 km away. These two earthquakes are the only two, out of 40 earthquakes, that fall within the Fleischer dislocation model (Fleischer, 1981). However, there are four other radon anomalies which also correspond to some earthquakes, even though these quakes do not conform to the dislocation model of Fleischer but are within the limits of error. These four anomalies are also shown in Figure 4.3b. The first event is a positive anomaly before the earthquake in week 6, but it is obscure because of the dominant 6.2M earthquake in week 7. The second event is a negative radon anomaly occurred about one week at 100-cm depth before the 2.5M earthquake in week 23. The third event is a positive radon anomaly occurred about three weeks at two depths before the 3.0M earthquake in week 30. The last event is a negative radon anomaly occurred about four weeks at two depths before the 4.0M

earthquake in week 36. The result of the comparison above is that radon anomalies at 100-cm depth correspond to every earthquakes but radon anomalies at 50-cm depth sometimes correspond to the earthquakes. These are discussed in chapter 5.

The abnormal behavior of radon before an earthquake may have two explanations. The first is that the increase in radon content is connected to the amount of porosity of a rock and, therefore, is sharply increased and then decreased before an earthquake due to closure of small pores. The second is that near the surface of the Earth, compression will cause upward flow of radon in pore spaces and tension will produce downward flow. Because of its short half life, transferal of radon over long distances is not possible. Since stress in an elastic body will produce strain everywhere, it follows that radon changes at studied sites are to be expected from local flow and diffusion that is caused by distant stress centers.

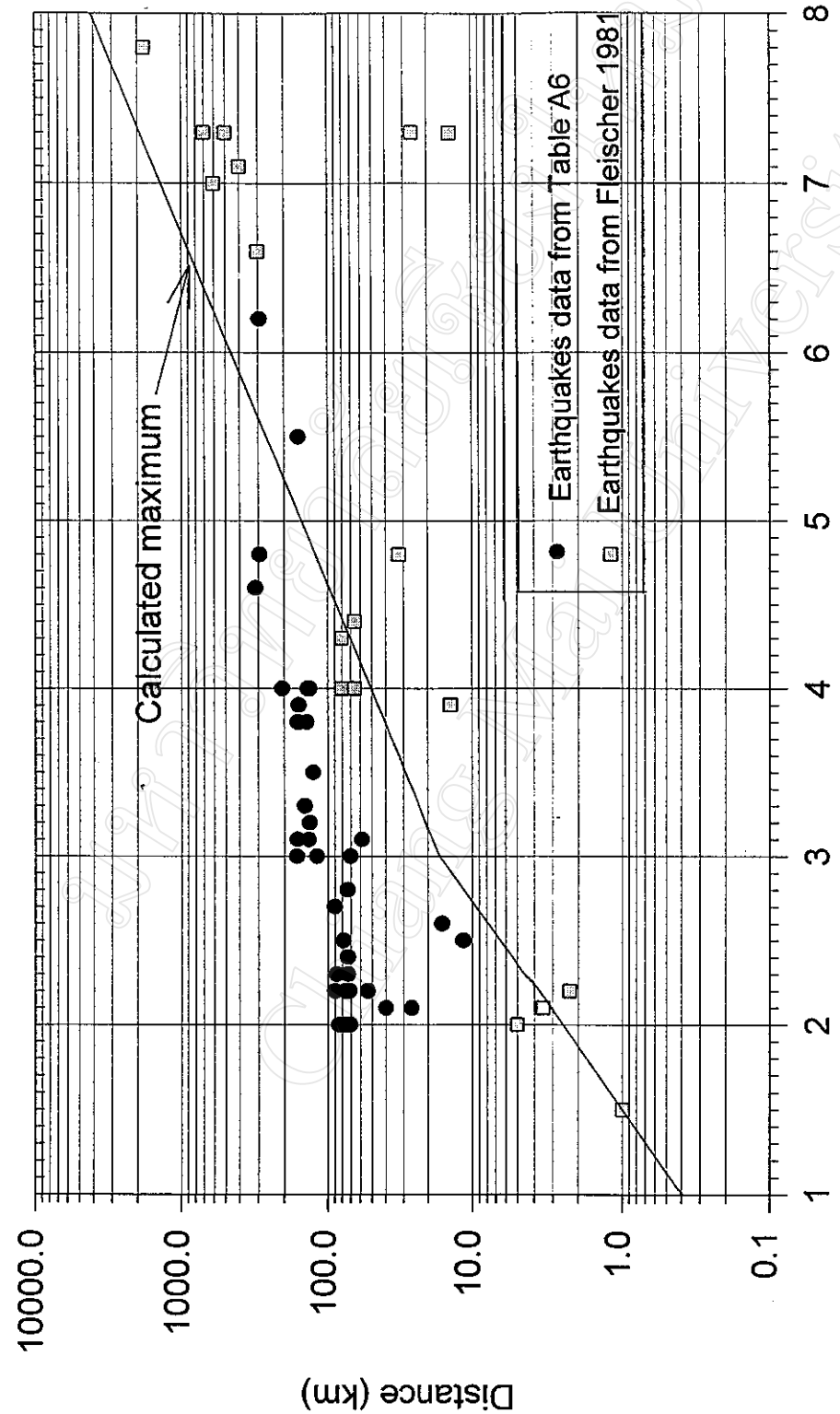

Figure 4.3a Calculated maximum distance vs magnitude.

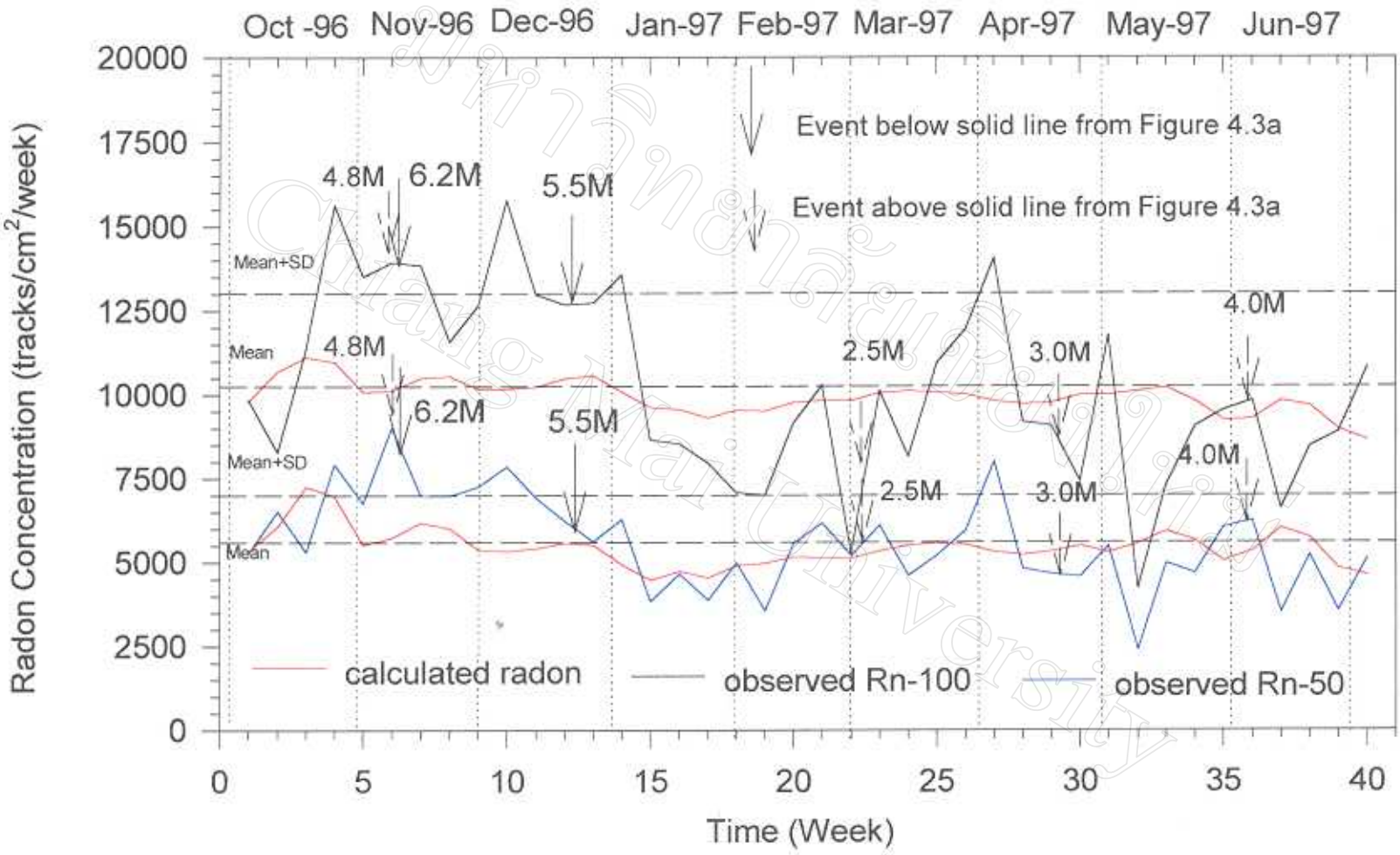

Figure 4.3b Compare radon data and earthquakes from disloation model of Fleischer.